RESEARCH REPORT

VTT-R-08604-11

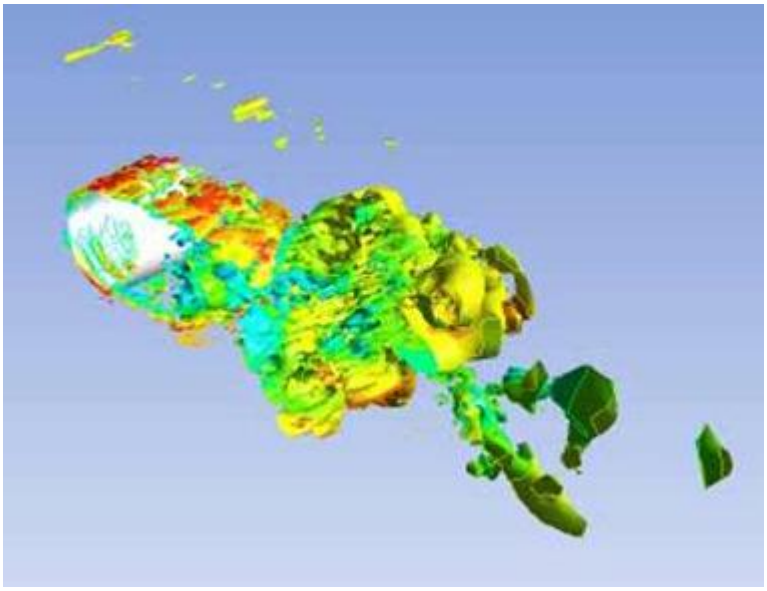

EFFIMA/SEEE/UNNO Deliverable

D2.2a Acoustic analogies in commercial programs

Authors: Seppo Uosukainen

Confidentiality: Public

Report's title	
D2.2a Acoustic Analogies in Commercial Programs	
Customer, contact person, address FIMECC Ltd / Tekes	Order reference
Project name Fimecc/Effima/2010/ISM – Unno	Project number/Short name 71112-1.4.2
Author(s) Seppo Uosukainen	Pages 12 p. + app. 15 p.
Keywords Noise, acoustic fields, flow, applicability	Report identification code VTT-R-08604-11

Summary

Actran uses Lighthill's analogy for calculating the aeroacoustic fields in a flowless medium and the Möhring's analogy in the case of convectional effects present. The calculations are based on the FEM formulation. LMS Virtual.Lab Aero-Acoustics Modeling uses Lighthill's analogy for calculating the aeroacoustic fields of volume distributed quadrupoles, Curle's analogy for calculating the fields of surface distributed dipoles, and the Ffowcs Williams–Hawkings analogy for calculating the fields of distributed fan sources (rotating fan). The radiated field is calculated using FEM or BEM technology. With Actran and LMS Virtual.Lab, the entropy variation parts and the viscous and thermal losses in the source terms are not included. Ansys Fluent and STAR-CCM+ offer a method based on the Ffowcs Williams–Hawkings analogy. The calculation process is essentially a boundary element method, only applicable in free space. With all programs using the Ffowcs Williams–Hawkings analogy, the Lighthill's stress dyadic, forming the volume distributed quadrupoles, is omitted. All the programs, presented here, can, in principle, be applied also to acoustic fields in liquids.

Confidentiality	Public

Espoo 1.12.2011

Written by	Reviewed by	Accepted by
Seppo Uosukainen Senior Scientist	Jukka Tanttari Principal Scientist	Johannes Hyrynen Deputy Technology Manager

VTT's contact address
Seppo Uosukainen, P.O. Box 1000, FI–02044 VTT, Finland

Distribution (customer and VTT)
Customer 1 copy (electronic)
VTT 1 copy

Preface

The work described in this publication has been carried out in VTT Smart Machines, Machinery and Environmental Acoustics Team. The results were obtained through the UNNO task (Underwater Noise) of the SEEE project (Ship's Energy Efficiency and Environment) in the EFFIMA programme (Energy and Lifecycle Efficient Machines) of FIMECC SHOK with funding from Tekes. The programme runs from 2009 to 2013. This report is based on a former report of this project "Foundations of acoustic analogies" [1], the aim of which was to present the best-known acoustic analogies and derive their equations mathematically in detail. The aim of this succeeding report is to continue that work to present the most important commercial programs that use acoustic analogies.

Espoo 1.12.2011

Author

Contents

1. Introduction

This report is based on a former report of this project “Foundations of acoustic analogies” [1], the aim of which was to present the best-known acoustic analogies and derive their equations mathematically in detail to clarify their applicability to calculating acoustic fields generated by flow and motion in flow, and to allow their applicability to be extended when necessary. The aim of this succeeding report is to continue that work to present the most important commercial programs that use acoustic analogies, and to present possible further assumptions and extensions of the analogies used by the programs, compared to the original formulations of the analogies.

The acoustic analogies are used to describe the connection between the flow and the sound field due to the flow, i.e., the dependence of the flow-generated sound on its causes (sources). In the acoustic analogies, the equations governing the acoustic fields are rearranged in such a way that the field variable connections (wave operator part) are on the left-hand side and that which is supposed to form the source quantities to the acoustic field (source part) is on the right-hand side, as

$$Lf = g\,, \tag{1}$$

where Lf is the wave operator part containing operator L and field f to be calculated, and g is the sources for field f. The right-hand side sources have to be known *a priori* or the field equation should be solved iteratively the source part becoming more accurate at every iteration loop. Apart from being based on different field variables, the various analogies differ from each other also with respect to the terms in the equations that are defined to form the right-hand side source quantities and the terms that are defined as belonging to the left-hand side, describing the behaviour of the field variable. [1]

Lighthill’s analogy is developed for unbounded flows with no static flow outside the source region and no refraction effects. Powell’s analogy is an approximate version of Lighthill’s analogy. The Ffowcs Williams–Hawkings analogy takes into account moving boundaries and Curle’s analogy takes into account stationary boundaries. In Phillips’ and Lilley’s analogies, the effects of a moving medium and the refraction effects are included. In Howe’s and Doak’s analogies, the vorticity and the entropy gradients play an important role as sources. The four last analogies assume that the medium is an ideal gas, so without modifications they cannot be applied to acoustic fields in liquids. [1]

The aeroacoustic fields are typically calculated with a hybrid two-step approach. The first step consists of the calculation of the turbulent flow field by some CFD (Computational Fluid Dynamics) program. This flow field is then used as input data for source definitions and this data has to be projected to the acoustic source terms for the CAA (Computational AeroAcoustics) calculations, mapping from the fine CFD to the coarser CAA mesh. The acoustic radiation is the computed with a CAA program, using as source for the noise generation the acoustic source terms evaluated from the flow computation. In this kind of hybrid methodology, no feedback from the acoustic field to the turbulent flow is considered [2].

The aeroacoustic field can, in principle, be calculated with a direct method, too. In the direct method, the turbulent flow and the sound generated by it are computed simultaneously. This is possible because both the flow and the acoustic field obey the same equations. The drawback of this method is that, because of very different length scales, it is computationally difficult and expensive inasmuch as it requires highly accurate numeric. It is feasible only in near-field calculations; the computational cost becomes prohitive for far-field calculations [3, 15.1.1]. Other drawbacks of this approach causing numerical difficulties are the much larger extent of the acoustic field compared with the flow field, the very small energy content of the acoustic field compared with the flow field, the possibility that the numerical discretization itself may act as a more significant source of sound than the flow field that is simulated, and the difficulty of imposing free space boundary conditions appropriate for the acoustics in far-field, at an artificial computational boundary positioned at a finite distance away from the source region [4].

In the next, the most important commercial programs that use acoustic analogies are presented. Most of them use the hybrid two-step method, so they need input data for source definitions from calculations done beforehand by some CFD program. The analogies used by the programs are presented. Further assumptions and extensions of the analogies used by the programs, compared to the original formulations of the analogies, are also presented.

The Möhring's analogy is presented and its equations are derived in Appendix F because it is not presented in [1] and it is used in Actran. Also in appendices are presented the principles of strong and weak forms of solutions for differential equations, and the principles of the variational and moment methods as weak forms because they are widely used with FEM models.

In this stage it should be mentioned that there are also CFD programs that directly generate proper source output for acoustic analogies, e.g., AcuSolve [5] produces the source terms for Lighthill's analogy and the Ffowcs Williams–Hawkings analogy. These kinds of programs are not treated here.

In some references of this report, the perturbation (fluctuating) fields are divided into hydrodynamic and acoustic fields. In the former report [1] of this project, this division has not been made and the perturbation fields have been defined to be equivalent to the acoustic fields. This is due to the fact that they obey just the same equations and this division is somehow confusing. Further, if sound is defined as pressure fluctuations around the static pressure, as it is normally done, all perturbation fields are in fact acoustic fields.

In this report it is assumed that the former report [1] is available for the reader so that references to its definitions, formulae and results can be utilized to support reading this report. As in the former report, the dyadic notation is used instead of the tensor notation, although the tensor notation is generally more widely used. This choice was made because, with the dyadic notation, the formulae are, in most cases, much simpler and more illustrative than with the tensor notation, at least for the author.

2. Programs using acoustic analogies

The programs studied and their versions are Actran 12, LMS Virtual.Lab Rev. 9 (LMS SYSNOISE Rev. 5.6), Ansys 13 Fluent and STAR CCM+ 6.02. Also with Actran, the transforming of the CFD data to CAA program is treated in more detail. Ansys Fluent and STAR CCM+ are actually CFD programs where an acoustic analogy has been implemented.

CFD data can be used to define loads to surfaces by some programs, e.g., Actran [6]. This is treated briefly in the end of Section 1.1. VaOne has an aero-vibro-acoustic module that can be used to add fluctuating surface pressure loads to structural subsystems in FEM, hydrodynamic boundary conditions in BEM, and data for fitting Corcos turbulent boundary layer model parameters, acoustic radiation into fluid adjacent the surfaces included. Input data is based on time domain CFD pressure data in formats of CGNS (*.cgns), Star-CD (*.ccm), IDEAS Universal (*.unv), Ensight (*.encas) or Fluent CASE (*.case), and the data is transformed into frequency domain before calculation [7, p. 8, 8, pp. 145–165]. These facilities are not directly involved with the acoustic analogies.

1.1 Actran

1.1.1 Used analogies

Actran uses Lighthill's analogy for calculating the aeroacoustic fields in a flowless medium and the Möhring's analogy in the case of convectional effects present. The acoustic volume source distributions have to be calculated beforehand with some CFD program [6, pp. 320–321]. The calculations are based on the FEM (Finite Element Method) formulation.

The input CFD data in time domain can be generated by Star-CD (*.ccmg, *.ccmt), Star-CCM+ (*.ccm), Fluent (*.cas, *.dat, *.cdat), Ensight-Gold (*.case), FINE/Turbo (*.cgns) or TRACE (*.cgns). All versions of the CFD codes do not produce compatible files to Actran. The aeroacoustic source terms are then calculated, transformed on the coarser acoustic mesh and transformed into frequency domain. Acoustic field calculation is then performed in frequency domain. [6, pp. 458–459, 464–465]

With Lighthill's analogy, the viscous and entropy effects in the volume source term $\overline{\overline{T}}_L$ (Lighthill's stress dyadic) [1, (5), (6)] are not taken into account, so only the Reynold's stress part $\overline{\overline{T}}_R$ of the dyadic is included in the source term [6, p. 461]

$$\overline{\overline{T}}_L \approx \overline{\overline{T}}_R = \rho \vec{U}\vec{U}\,, \tag{2}$$

where ρ is density and $\vec{U}$ is the velocity. The Lighthill's equation is used in the weak moment method (weighted residual method) formulation (C.7) [6, p. 324]. The weak formulation used needs the density and the normal component of velocity at boundaries as extra source quantities. These are needed with interfaces between finite and infinite element domains, vibrating walls and permeable surfaces (boundaries for the acoustic problem but not for the CFD simulation, e.g., inter-

face between rotating and static CFD domains). With non-moving boundaries these are not needed [6, p. 461]. The formulation does not use sound pressure as a field quantity (as used in Appendix C) but a potential function related to the perturbation density [6, p. 323]. The weak formulation for the Lighthill's equation was first derived by Oberai *et al.* [9, 10].

With Möhring's analogy, the entropy variation parts in the volume source term, see Eq. (F.18), are not included [6, p. 463]. The Möhring's equation is used in the weak moment method formulation [6, p. 312]. Also with this weak formulation, the density and the normal component of velocity at boundaries as extra source quantities are needed. It is stated in Actran User's Guide, that the viscous stresses are accounted in the close vicinity of walls by the boundary integral of the weak formulation (not in the volume integral) [6, p. 463]. This seems to be the case according to Eqs. [6, (23.7), (23.26)]. The derivation of the first equation (23.7) is not based on the original form of Möhring's analogy as in Eq. (F.18) [11, 12], but in the form of Eq. (F.17) which takes the viscous and thermal losses into account (without entropy variations). However, part of the loss terms, namely f_d, where

$$f_d = \nabla \cdot \left(\vec{U} \cdot \overline{\overline{\sigma}}_\mu + K \nabla T \right), \tag{3}$$

where $\overline{\overline{\sigma}}_\mu$ is the viscous part of the stress dyadic, K is the thermal conductivity and T is the temperature, is omitted [6, p. 307]. So the viscous losses are not rigorously taken into account in the boundary integral.

With Actran it is also possible to use wall pressure fluctuations to load mechanically a structure and to use mean aerodynamic fields in a convected propagation analysis, both computed by a CFD code. The same input data formats than with the acoustic analogies are compatible, and with the convected propagation analysis input CFD data can be generated by I-deas (*.unv), Tecplot (*.tecplot) and Actran (*.nff, *.dat). [6 , pp. 457–458, 464–465, 482]

Actran DGM is designed for predicting the propagation of tonal engine noise components in a moving fluid with shear layers and in the presence of acoustically lined ducts, typically engine nacelle exhausts. It has a FWH Utility after the names of Ffowcs Williams and Hawkings. This utility is not involved with the Ffowcs Williams–Hawkings analogy but only the same notation in frequency domain is used to present the sound field by equivalent moving Huygens' source surface enclosing a source volume. The physical sources inside the surface can be monopoles or coupling with acoustic duct modes. Aerodynamic CFD data cannot be used as sources. [13, pp. 19, 302–304, 321–322, 283]

1.1.2 Transforming CFD results to Actran

Actran has a utility named iCFD that allows, e.g., the computation of the aeroacoustic sources from CFD data of formely defined CFD codes, for the application of Lighthill's or Möhring's analogies. ICFD can read time domain pressure, density, velocity and temperature field output of a CFD solver. The same utility is used for the computation of wall pressure fluctuations and mean aerodynamic fields. For aeroacoustic calculations, the CFD source data should consist of density and velocity for compressible CFD computation and velocity for incompressi-

ble CFD computation. The aeroacoustic source terms are then calculated in time domain using oversampling by default at every half CFD time steps to avoid aliasing effects during the Fourier transform, and saved in a NFF database. The time step for oversampling can be defined and should be done, e.g., as one third CFD time step for compressible CFD computation. The starting and ending times for iFCD calculation can be defined. The calculated aeroacoustic source terms are the transformed on the (typically) coarser acoustic mesh by sampling (iCFD identifies the closest CFD cell to each acoustic node) or by integrating over the CFD mesh using the shape functions of the acoustic mesh, the latter being the default approach. Finally the time data in CAA model is transformed into frequency domain. Acoustic field calculation is then performed in frequency domain. The procedure above holds also to wall pressure fluctuation calculations, the CFD pressure data being the starting point in that case. [6, pp. 457–468, 480]

With the convected propagation analysis, the mean velocity, density, pressure, temperature and speed-of- sound fields from the steady CFD results can be interpolated to the acoustic mesh. Also the unsteady CFD results can be used in which case an average of the mean aerodynamic fields over the available time steps is first performed. With the regularization process, unmapped points (see definition a little below) and flow boundary conditions can be accounted. The regularization process enables to set values at unmapped points based on the mean flow values in their vicinity. The projected mean flow at selected surfaces is corrected based on the mean flow in their neighbourhood and the mean flow velocity normal to the boundary is set to zero by the regularization process, to ensure a correct usage of the Myers boundary condition. With the regularization process, the quality of the mapping can be improved when the CFD mesh is coarser than the CAA mesh by smoothing the mean flow. [6, pp. 480–485]

ICFD can also automatically rotate or translate the CAA model in order to put it in the same coordinate system than the CFD model [6, p. 469]. In the case of coarse CFD surface mesh, it can be artificially refined to improve the quality of the integration of the surface sources [6, p. 467].

During the projection process, the nodes of the Actran model are localized in the CFD mesh. For a given node, this involves the identification of the element of the CFD mesh containing the node and the computation of its local coordinates within the CFD element. If the node does not belong to any finite element, it is said to be unmapped. The unmapped nodes can be handled by successive in-plane tolerances. The localization process is first launched using the first planar tolerance. If unmapped points are detected, the projection process is launched a second time, on this set of unmapped point, with the second planar tolerance, which should therefore be less strict than the first one. The tolerance is interpreted as the relative amount by which the point may be located outside of a CFD element. This iterative refinement continues until there are no more unmapped points or the list of planar tolerances has been completely used. [6, p. 488]

1.2 LMS Virtual.Lab

LMS Virtual.Lab Aero-Acoustics Modeling uses Lighthill’s analogy for calculating the aeroacoustic fields of volume distributed quadrupoles, Curle’s analogy for calculating the fields of surface distributed dipoles, and the Ffowcs Williams–Hawkings analogy for calculating the fields of distributed fan sources (rotating

fan). The aero-acoustic volume and boundary source quantities have to be calculated beforehand with some CFD program. LMS Virtual.Lab then calculates the resulting radiated field using FEM or BEM technology, including scattering effects (reflection and diffraction). [14]

The input CFD data can be generated by leading CFD codes (FLUENT, STAR-CD, STAR-CCM, CFX, Powerflow, CFD++, SkryuTetra, FineTurbo, etc.). The input data can be either in time domain or in frequency domain and the time domain data is first transformed to frequency domain. Data is mapped typically from the fine CFD to the coarser acoustic mesh. The CFD and CAA meshes can be compatible, have same geometry and different densities, or have different geometries and different densities [14, 15, pp. 5–146, 150–153]. In the present version, the input data for fan sources has to be specified [15, p. 5–155].

With Lighthill's analogy, the viscous and entropy effects in the quadrupole source term $\overline{\overline{T}}_L$ (Lighthill's stress dyadic) in [1, (4), (5), (6)] are not taken into account, so only the Reynold's stress part $\overline{\overline{T}}_R$ of the dyadic is included in the volume source term [15, p. 5–124], as with Actran, see Eq. (2). The incident (free) field is calculated using Green's functions [1, (F1), last expression] in frequency domain [15, pp. 5–124, 5–151] and scattered fields due to boundaries are separately included in the calculation. Lighthill's analogy is available in FEM and BEM.

With Curle's analogy, the Lighthill's stress dyadic is used as with Lighthill's analogy stated above. The viscous effects in the equivalent dipole distribution $\vec{f}_{WS}$ in [1, (31), (18)] are not taken into account, so this surface source term, due to flow, is used as [15, p. 5–125]

$$\vec{f}_{WS} = p\vec{e}_n, \tag{4}$$

where p is the pressure on the dipole surface, due to flow and calculated by compressible CFD, and $\vec{e}_n$ is a unit normal vector on the surface pointing towards the space under consideration. Also incompressible CFD calculations can be used as a starting point in which case acoustic pressure can be included in the dipole surface term (4) to take acoustic scattering at the surface into account [16]. The field due to Lighthill's stress dyadic is calculated as with Lighthill's analogy using Green's functions in frequency domain. The field of the surface dipole distribution is also calculated using Green's functions [1, (F1), second expression] in frequency domain [15, pp. 5–125, 5–144]. Curle's analogy is available in BEM.

With the Ffowcs Williams–Hawkings analogy, the Lighthill's stress dyadic $\overline{\overline{T}}_L$ and the equivalent surface monopole distribution q_{WS} in [1, (13)] are omitted, see [15, p. 5–137], and the equivalent surface dipole distribution $\vec{f}_{WS}$, due to flow, is as in Eq. (4). So it is assumed that the dipole source part on the impermeable surface [1, (18)] dominates the sound radiation and its viscous part can be omitted. The analogy can be used for equivalent "rotating dipoles" for predicting the fan radiated noise at the blade passing frequency and its harmonics [14]. The broadband noise is not calculated. The analogy is available in FEM and BEM.

1.3 Ansys Fluent

Ansys Fluent offers three approaches to computing aerodynamically generated noise; a direct method, an integral method based on acoustic analogy and a method that utilizes broadband noise source models [3, 15.1]. With the acoustic analogy, Ansys Fluent calculates the CFD data needed by itself, because it is actually a CFD program where the acoustic analogy has been implemented.

Ansys Fluent offers a method based on the Ffowcs Williams–Hawkings analogy [1, (13)] with the last term in the right-hand side of the equation (effect of Lighthill's stress dyadic) omitted [3, 15.2.1], taking into account only equivalent surface monopole and dipole sources as in Eqs. [1, (15) & (16)]. The acoustic field calculations are done in time domain, based on time-accurate solutions of the flow-field variables. The results can be processed into frequency domain. The calculations can be done only to free space, no external boundaries can be present [3, 15.1.2]. The calculations are based on direct surface integrals based on Farassat's formulation 1A of the integral presentation of the Ffowcs Williams–Hawkings equation using the free space Green's function [18, 19]. That formulation is based on equations [1, (24) & (27)] and in the method used the spatial derivatives have been transformed to temporal ones and the latter are inserted into the surface integrals. The calculation process is essentially a boundary element method (BEM). The surfaces of integration need not to be physical source surfaces, they can be any surfaces enclosing source distributions. The effects of the Lighthill's stress dyadic can be taken into account if this distribution is enclosed by the surfaces of integration [3, 15.1.2].

1.4 STAR-CCM+

STAR-CCM+ offers a method based on the Ffowcs Williams–Hawkings analogy [17]. With the acoustic analogy, STAR-CCM+ calculates the CFD data needed by itself, because it is actually a CFD program where the acoustic analogy has been implemented.

The Ffowcs Williams–Hawkings analogy [1, (13)] is used similarly as with Ansys Fluent [4].

3. Conclusions

In this report the most important commercial programs that use acoustic analogies, and further assumptions and extensions of the analogies used by the programs, compared to the original formulations of the analogies, are presented. With Actran and LMS Virtual.Lab, the acoustic source distributions have to be calculated beforehand with some CFD program. With Ansys Fluent and STAR-CCM+, the CFD data needed is calculated by the programs themselves, because they are actually CFD programs where the acoustic analogy has been implemented. All the programs, presented here, can, in principle, be applied also to acoustic fields in liquids. The author is not aware about any applications of propeller noise in water.

Actran uses Lighthill's analogy for calculating the aeroacoustic fields in a flowless medium and the Möhring's analogy in the case of convectional effects present. The calculations are based on the FEM formulation. With Lighthill's analo-

gy, the viscous and entropy effects in the volume source term (Lighthill's stress dyadic) are not taken into account, so only the Reynold's stress part of the dyadic is included in the source term. With Möhring's analogy, the entropy variation parts and the viscous and thermal losses in the volume source term are not included.

LMS Virtual.Lab Aero-Acoustics Modeling uses Lighthill's analogy for calculating the aeroacoustic fields of volume distributed quadrupoles, Curle's analogy for calculating the fields of surface distributed dipoles, and the Ffowcs Williams–Hawkings analogy for calculating the fields of distributed fan sources (rotating fan). LMS Virtual.Lab calculates the radiated field using FEM or BEM technology. With Lighthill's analogy, the viscous and entropy effects in the volume source term (Lighthill's stress dyadic) are not taken into account, as with Actran. With Curle's analogy, the Lighthill's stress dyadic is used similarly, and the viscous effects in the equivalent dipole distribution are not taken into account. With the Ffowcs Williams–Hawkings analogy, the Lighthill's stress dyadic and the equivalent surface monopole distribution are omitted, and the equivalent surface dipole distribution is used as in Curle's analogy.

Ansys Fluent and STAR-CCM+ offer a method based on the Ffowcs Williams–Hawkings analogy. The analogy is used with the effect of Lighthill's stress dyadic omitted, taking into account only equivalent surface monopole and dipole sources. The calculations are based on free space Green's function, so the calculation process is essentially a boundary element method. The calculations can be done only to free space, no external boundaries can be present.

4. Summary

Actran uses Lighthill's analogy for calculating the aeroacoustic fields in a flowless medium and the Möhring's analogy in the case of convectional effects present. The calculations are based on the FEM formulation. LMS Virtual.Lab Aero-Acoustics Modeling uses Lighthill's analogy for calculating the aeroacoustic fields of volume distributed quadrupoles, Curle's analogy for calculating the fields of surface distributed dipoles, and the Ffowcs Williams–Hawkings analogy for calculating the fields of distributed fan sources (rotating fan). The radiated field is calculated using FEM or BEM technology. With Actran and LMS Virtual.Lab, the entropy variation parts and the viscous and thermal losses in the source terms are not included. Ansys Fluent and STAR-CCM+ offer a method based on the Ffowcs Williams–Hawkings analogy. The calculation process is essentially a boundary element method, only applicable in free space. With all programs using the Ffowcs Williams–Hawkings analogy, the Lighthill's stress dyadic, forming the volume distributed quadrupoles, is omitted. All the programs, presented here, can, in principle, be applied also to acoustic fields in liquids.

References

1. Uosukainen, S. Foundations of acoustic analogies. VTT Publications 757. Espoo: VTT. 2011. 34 p. + app. 69 p.
2. Escobar, M. Finite Element Simulation of Flow-Induced Noise using Lighthill's Acoustic Analogy. Erlangen: Universität Erlangen–Nürnberg. 2007. 137 p.

3. Ansys 13.0 Help – Fluent – Theory Guide. Ansys, Inc. 2010.
4. Caraeni, M., Aybay, O. & Holst, S. Tandem cylinder and idealized side mirror far-field noise predictions using DES and an efficient implementation of FW–H equation. 17th AIAA/CEAS Aeroacoustics Conference, 05–08 June 2011. Portland, Oregon.
5. AcuSolve – Command Reference Manual, Version 1.7. http://www.acusim.com/doc/OLD/command_reference.pdf
6. ACTRAN 12 User's Guide. Volume 1: Installation, Operations, Theory and Utilities. Free Field Technologies SA. 2011. 585 p.
7. VaOne 2010.5 Release Notes. Esi Group, Apr-11.2011.
8. VaOne 2010.5 Tutorials Guide. Esi Group, Apr-11.2011.
9. Oberai, A. A., Roknaldin, F. & Hughes, T. J. R. Computational procedures for determining structural-acoustic response due to hydrodynamic sources. Comput. Methods Appl. Mech. Engrg. 2000. Vol. 190, pp. 345–361.
10. Oberai, A. A., Roknaldin, F. & Hughes, T. J. R. Computation of trailing-edge noise due to turbulent flow over an airfoil. AIAA Journal 2002. Vol. 40, No. 11, pp. 2206–2216.
11. Möhring, W. A well posed acoustic analogy based on a moving acoustic medium. Aeroacoustic workshop SWING. Dresden 1999.
12. Möhring, W. A well posed acoustic analogy based on a moving acoustic medium. Available at http://arxiv.org/PS_cache/arxiv/pdf/1009/1009.3766v1.pdf.
13. ACTRAN DGM 12 User's Guide. Free Field Technologies SA. 2011. 350 p.
14. LMS product information. LMS Virtual-Lab Rev 9. LMS Virtual.Lab Aero-Acoustic Modeling [VL-ACM.41.3].
15. LMS SYSNOISE Rev 5.6, Model data.
16. Schram, C. A boundary element extension of Curle's analogy for non-compact geometries at low-Mach numbers. J. Sound Vib. 2009. Vol. 322, No. 1–2, pp. 264–281.
17. STAR-CCM+ V5.06: Now with Discrete Element modelling. Available at http://www.cd-adapco.com/news/2010/29-10-starccmplus506.html.
18. Farassat, F. & Brentner, K. S. The acoustic analogy and the prediction of the noise of rotating blades. Theoret. Comput. Fluid Dynamics 1998. Vol. 10, pp. 155–170.
19. Brentner, K. S. Prediction of Helicopter Rotor Discrete Frequency Noise – A Computer Program Incorporating Realistic Blade Motions and Advanced Acoustic Formulation. NASA Technical Memorandum 87721. Washington DC: National Aeronautics and Space Administration, 1986. 93 p.
20. Fahy, F. & Gardonio, P. Sound and Structural Vibration. Radiation, Transmission and Response. Amsterdam: Academic Press. 2007. 633 p.
21. Akin, J. E. Finite Element Analysis for Undergraduates. London: Academic Press. 1986. 319 p.
22. Van Bladel, J. Electromagnetic fields. Washington: Hemisphere. 1985. 556 p.
23. Lindell, I. Sähkömagnetiikan likimääräismenetelmät. Luentomoniste. Espoo: TKK. 1978. 148 s.
24. Gladwell, G. M. & Zimmermann, G. On energy and complementary energy formulations of acoustic and structural vibration problems. J. Sound Vib. 1966. Vol. 3, No. 3, pp. 233–241.
25. Bathe, K.-L. Finite Element Procedures in Engineering Analysis. New Jersey: Prentice–Hall, Inc. 1982. 735 p.
26. Harrington, R. F. Field Computation by Moment Methods. New York: The Macmillan Company. 1968. 229 p.
27. Baker, A. J. & Pepper, D. W. Finite Elements 1–2–3. New York: McGraw–Hill, Inc. 1991. 341 p.

Appendix A: Principles of strong and weak forms

Strong form

Consider a deterministic problem where field f is governed by a differential equation

$$Lf = g\,, \tag{A.1}$$

where L is the wave operator and g is the sources for field f. Let the boundary conditions be presented as

$$Bf = s \text{ at boundary,} \tag{A.2}$$

where B is the boundary condition operator

.

The equations above state the field problem in a "strong form" because they have to be fulfilled in every point in the medium and its boundary.

Weak form

The problem can be defined in a "weak form" if the field equation and the boundary condition are met only in an average sense by considering an integral expression of a function that implicitly contains the field equation and the boundary condition [20]. That can be done, e.g., with the variational methods or the moment methods (weighted residual methods).

The earliest mathematical formulations for finite element models were based on variational techniques. Variational techniques still are very important in developing elements and in solving practical problems. This is especially true in the areas of structural mechanics and stress analysis. The generation of finite element models by the utilization of weighted residual techniques is a relatively recent development (citation from 1986). However, these methods are increasingly important in the solution of differential equations and other non-structural applications. [21]

In the next, a symmetric inner product of u and v in a volume V is utilized and in a 3-D space it is defined as a volume integral

$$(u,v) = \int_V uv\,\mathrm{d}V\,. \tag{A.3}$$

Also an inner product at the boundary surface S of the space is defined as a surface integral

$$(u,v)_S = \oint_S uv\,\mathrm{d}S\,. \tag{A.4}$$

Variational methods

In the variational methods one tries to form a proper functional J of the field quantities in such a way that the functional is stationary. A functional is a mapping from a function to a scalar. A functional is stationary with a function f_0 if the change in the value of the functional, caused by a small change δf in the function, is of the second order. Setting the variation of a stationary functional to zero gives the field function.

One general functional, the "energy functional", is suitable for deterministic self-adjoint problems. It can be presented as [22, 23]

$$J(f) = 2(f, g) - (f, Lf) + 2(Cf, s)_S - (Cf, Bf)_S . \tag{A.5}$$

Operator C above can be identified from the Green's second identity

$$(Lf, h) + (Bf, Ch)_S = (f, L^a h) + (C^a f, B^a h)_S , \tag{A.6}$$

where h is an other field function and operators with a superscript a are corresponding field operators of the adjoint problem. With self-adjoint problems

$$L^a = L \quad B^a = B \quad C^a = C . \tag{A.7}$$

In practice, Eq. (A.6) is obtained and the corresponding operators can be found by partial integration of term (Lf,h).

In the frequency domain the energy functional is better expressed as

$$J(f) = 2(f, g^*) - (f, (Lf)^*) + 2(Cf, s^*)_S - (Cf, (Bf)^*)_S , \tag{A.8}$$

where the asterisk means complex conjugate.

The weak formulation can be further developed by using Green's identities. By their help the orders of the spatial derivatives can be lowered. This is beneficial because the trial functions need not to have so many continuous derivatives. This is illustrated in Appendix B for the Lighthill's equation.

In Appendix B is presented the energy functional in time harmonic field of the Lighthill's equation when the boundary is taken into account by velocity boundary condition. In that case the energy functional is deduced to a form which is composed of the effect of the source distribution (Lighthill's stress dyadic), Lagrangian energy of the field and the work done to the fluid by the boundary vibration. That is one version of the Hamilton's principle where the Lagrangian energy E_L plays an important role [24]

$$E_L = T - U , \tag{A.9}$$

where T and U denote, respectively, the kinetic and potential energies of the system. According to the Hamilton's principle among all displacements which satisfy the prescribed conditions at times $t = t_1$ and $t = t_2$, the actual solution satisfies the equation

$$\delta J = \int_{t_1}^{t_2} \left(\delta E_L + \delta W_{nc} \right) \mathrm{d}t = 0 \ , \tag{A.10}$$

where δW_{nc} is the virtual work done by the non-conservative forces (external sources, forces and moments, dissipation forces and moments) [20]. The energies and the virtual work are associated to the whole medium in consideration, so volume integrations are needed in the Hamilton's principle. If the equation of the Hamilton's principle can be solved analytically, the exact solution of the problem can be obtained. If this is not the case, e.g., when predetermined functions are used to seek the solution, only an approximate solution is generally achieved.

In Rayleigh-Ritz method, the field f is approximated with a predetermined set of shape functions ϕ_i which are dependent of spatial coordinates

$$f = \sum_{i=1}^{N} \alpha_i(t) \phi_i(\vec{r}) + R_f \, , \tag{A.11}$$

where R_f is the error of f, being orthogonal to the set of shape functions. The time dependent factors α_i (generalized coordinates) can be calculated from equations [25]

$$\frac{\partial}{\partial \alpha_j} J\left(\sum_{i=1}^{N} \alpha_i \phi_i \right) = 0, \ j = 1 \ldots N \, . \tag{A.12}$$

In order to guarantee convergence to the exact solution, the shape functions must be linearly independent, be differentiable sufficiently times to be inserted into the Hamilton's principle or into another stationary functional, and form a complete set (the exact solution is approached arbitrarily close by increasing the number of shape functions) [20].

Moment methods

In the moment methods (method of moments, weighted residual methods) [26] the weak formulation is done without forming any functionals. Despite of that, some categorize these methods to the variational methods.

In the moment methods, the differential (or integral) field equation is directly treated. The field f is approximated with a predetermined set of basis functions (expansion functions, trial functions) ϕ_i so that

$$f \approx f_\phi = \sum_{i=1}^{N} \alpha_i \phi_i \, . \tag{A.13}$$

The residual for the field equation is thus

$$R = Lf - Lf_\phi = g - \sum_{i=1}^{N} \alpha_i L\phi_i \,. \tag{A.14}$$

Also a residual for the boundary condition is obtained

$$R_s = Bf - Bf_\phi = s - \sum_{i=1}^{N} \alpha_i B\phi_i \text{ at boundary.} \tag{A.15}$$

Let volume V be the medium under consideration. In the moment methods, a set of weight functions (test functions) w_j ($j = 1\ldots N$) is selected and the inner product of the residual with each of the weight functions is demanded to disappear

$$\begin{aligned} \left(w_j, R\right) &= \left(w_j, g - \sum_{i=1}^{N} \alpha_i L\phi_i \right) \\ &= \left(w_j, g\right) - \left(w_j \sum_{i=1}^{N} \alpha_i L\phi_i \right) = 0, \; j = 1\ldots N \,. \end{aligned} \tag{A.16}$$

This gives N equations to solve the unknown factors α_i. The residual is orthogonal to the set of the weight functions. Part of the weight functions can be selected to weight the residual of the boundary condition also. The inner product for the boundary condition is a surface integral.

The weak formulation can be further developed by using Green's identities. By their help the orders of the spatial derivatives can be lowered. This is beneficial because the basis functions need not to have so many continuous derivatives. This is illustrated in Appendix C for the Lighthill's equation.

The moment methods can further be divided into submethods, based on the selection of the weight function set. Some of them are presented below.

In the Galerkin method [25, 26, 27, 21], the weight functions are selected to be the same as the basis functions

$$w_j = \phi_j \,. \tag{A.17}$$

With self-adjoint problems this leads to the same results than the Rayleigh–Ritz variational formulation [23, 27].

In the least squares method [25, 23], the weight function are selected so that

$$w_j = \left(L\phi_j\right)^* \,, \tag{A.18}$$

and the norm of the residual (R^*,R) will be minimized.

In the collocation method (point-matching method) [25, 26, 21], the weight functions are selected as Dirac delta functions

$$w_j = \delta(\vec{r} - \vec{r}_j), \tag{A.19}$$

and the residual is thus set to zero at N points.

In the subdomain method [25, 21], the medium under consideration is divided into subdomains V_j and the weight functions are selected to be pulse functions

$$w_j = \begin{cases} 1 & \text{inside } V_j \\ 0 & \text{outside } V_j \end{cases} \tag{A.20}$$

to get the residual to vanish in each subdomain.

Appendix B: Energy functional of Lighthill's analogy in frequency domain

The equation of Lighthill's analogy is [1, (4) & (3)]

$$\frac{1}{c^2}\frac{\partial^2 p}{\partial t^2} - \nabla^2 p = \nabla\nabla : \overline{\overline{T}}_L , \tag{B.1}$$

where p is the sound pressure, c is the local speed of sound in constant entropy, t is time, and $\overline{\overline{T}}_L$ is the Lighthill's turbulence stress dyadic (or traditionally tensor).

In frequency domain the equation is

$$\nabla^2 p + k^2 p = -\nabla\nabla : \overline{\overline{T}}_L , \tag{B.2}$$

where $k = \omega/c$.

The general energy functional (A.8) can be presented for the Lighthill's equation by the help of Appendix D as

$$\begin{aligned} J(p) = &-2\int_V p\left(\nabla\nabla : \overline{\overline{T}}_L\right)^* \mathrm{d}V - \int_V p(\nabla^2 + k^2)p^* \,\mathrm{d}V \\ &+ 2\oint_S \mathrm{j}\omega\rho p v^* \,\mathrm{d}S + \oint_S p\vec{e}_n \cdot (\nabla p)^* \,\mathrm{d}S . \end{aligned} \tag{B.3}$$

The energy functional can be further developed by the Green's first identity. By its help the second order spatial derivatives can be changed to first order ones. This is beneficial because the trial functions need not to have so many continuous derivatives. By the help of Eq. (E.2) we obtain

$$-2\int_V p\left(\nabla : \overline{\overline{T}}_L\right)^* \mathrm{d}V = -2\oint_S p\vec{e}_n \cdot \left(\nabla \cdot \overline{\overline{T}}_L\right)^* \mathrm{d}S + 2\int_V \nabla p \cdot \left(\nabla \cdot \overline{\overline{T}}_L\right)^* \mathrm{d}V . \tag{B.4}$$

Similarly, by the help of Eq. (E.1) we obtain

$$-\int_V p\left(\nabla^2 p\right)^* \mathrm{d}V = -\oint_S p\vec{e}_n \cdot (\nabla p)^* \,\mathrm{d}S + \int_V \nabla p \cdot (\nabla p)^* \,\mathrm{d}V . \tag{B.5}$$

The energy functional (B.3) can be presented by the help of Eqs. (B.4) and (B.5) in the following alternative formulae

$$
\begin{aligned}
J(p) &= 2\int_V \nabla p \cdot \left(\nabla \cdot \overline{\overline{T}}_L\right)^* \mathrm{d}V - 2\oint_S p\vec{e}_n \cdot \left(\nabla \cdot \overline{\overline{T}}_L\right)^* \mathrm{d}S \\
&\quad - \int_V k^2 |p|^2 \,\mathrm{d}V + \int_V |\nabla p|^2 \,\mathrm{d}V + 2\oint_S \mathrm{j}\omega\rho p v^* \,\mathrm{d}S \\
&= 2\int_V \nabla p \cdot \left(\nabla \cdot \overline{\overline{T}}_L\right)^* \mathrm{d}V - 2\oint_S p\vec{e}_n \cdot \left(\nabla \cdot \overline{\overline{T}}_L\right)^* \mathrm{d}S \\
&\quad + 2\rho\omega^2 \left(\int_V \frac{\rho}{2} \left| \frac{\nabla p}{\rho\omega} \right|^2 \mathrm{d}V - \int_V \frac{1}{2\rho c^2} |p|^2 \,\mathrm{d}V + \oint_S p \left(\frac{v}{\mathrm{j}\omega} \right)^* \mathrm{d}S \right) \\
&= 2\int_V \nabla p \cdot \left(\nabla \cdot \overline{\overline{T}}_L\right)^* \mathrm{d}V - 2\oint_S p\vec{e}_n \cdot \left(\nabla \cdot \overline{\overline{T}}_L\right)^* \mathrm{d}S + 2\rho\omega^2 \left(E_L + W\right),
\end{aligned}
\tag{B.6}
$$

where E_L is the Lagrangian energy (difference between kinetic and potential energies) and W is the work done by the boundary

$$
\begin{aligned}
E_L &= T - V \\
T &= \int_V \frac{\rho}{2} |\vec{u}|^2 \,\mathrm{d}V \\
V &= \int_V \frac{1}{2\rho c^2} |p|^2 \,\mathrm{d}V \\
W &= \oint_S p\zeta^* \,\mathrm{d}S \\
\vec{u} &= \frac{\nabla p}{\mathrm{j}\omega\rho} \\
\zeta &= \frac{v}{\mathrm{j}\omega},
\end{aligned}
\tag{B.7}
$$

where T is the kinetic energy, V is the potential energy, $\vec{u}$ is the acoustic particle velocity and ξ is the normal component of the displacement of the boundary.

The energy functional is thus composed of the effect of the source distribution (Lighthill's stress dyadic), Lagrangian energy of the field and the work done to the fluid by the boundary vibration.

Appendix C: Weak moment method formulation of Lighthill's analogy

The equation of Lighthill's analogy is [1, (4) & (3)]

$$\frac{1}{c^2}\frac{\partial^2 p}{\partial t^2} - \nabla^2 p = \nabla\nabla : \overline{\overline{T}}_L , \tag{C.1}$$

where p is the sound pressure, c is the local speed of sound in constant entropy, t is time, and $\overline{\overline{T}}_L$ is the Lighthill's turbulence stress dyadic (or traditionally tensor).

According to Appendix A, Eqs. (A.16), (A.3) and (A.13), the weak formulation with the moment method for the Lighthill's equation is

$$\begin{gathered}\int_V w_j \nabla\nabla : \overline{\overline{T}}_L dV - \int_V w_j \left(\frac{1}{c^2}\frac{\partial^2 p_\phi}{\partial t^2} - \nabla^2 p_\phi \right) \mathrm{d}V = 0,\ j = 1 \ldots N \\ p_\phi = \sum_{i=1}^{N} \alpha_i \phi_i \ .\end{gathered} \tag{C.2}$$

This can be presented in a more convenient form by utilizing the Green's first identity, Appendix E. By its help the second order spatial derivatives can be changed to first order ones. This is beneficial because the basis functions need not to have so many continuous derivatives.

According to Eq. (E.1) one can write

$$\int_V w_j \nabla^2 p_\phi \, \mathrm{d}V = \oint_S w_j \vec{e}_n \cdot \nabla p_\phi \, \mathrm{d}S - \int_V \nabla\left(w_j\right) \cdot \nabla p_\phi \, \mathrm{d}V \ . \tag{C.3}$$

Similarly according to Eq. (E.2)

$$\int_V w_j \nabla\nabla : \overline{\overline{T}}_L \, \mathrm{d}V = \oint_S w_j \vec{e}_n \cdot \nabla \cdot \overline{\overline{T}}_L \, \mathrm{d}S - \int_V \nabla w_j \cdot \nabla \cdot \overline{\overline{T}}_L \, \mathrm{d}V \ . \tag{C.4}$$

Utilizing Eqs. [1, (5)] and [1, (6)] we have

$$\begin{aligned}\nabla \cdot \overline{\overline{T}}_L + \nabla p &= \nabla \cdot \left[\rho \vec{U}\vec{U} + \left(p - c^2 \rho'\right) \bar{\mathrm{I}} - \overline{\overline{\sigma}}'_\mu \right] + \nabla p \\ &= \nabla \cdot \left[\rho \vec{U}\vec{U} + p \bar{\mathrm{I}} - \overline{\overline{\sigma}}'_\mu \right] - \rho' \nabla c^2 \ ,\end{aligned} \tag{C.5}$$

where ρ' is the perturbation component of the density ρ, $\vec{U}$ is the particle velocity, $\bar{\mathrm{I}}$ is the identic dyadic, $\overline{\overline{\sigma}}'_\mu$ is the perturbation component of the viscous part of the stress dyadic $\overline{\overline{\sigma}}_\mu$. When there are no mass, force or momentum source dis-

tributions, and when the sound speed and the static parts of the pressure and the viscous stress dyadic change not very much as functions of the spatial coordinates, this can be further written according to Eq. [1, (B.4)] as

$$\nabla \cdot \overline{\overline{T}}_L + \nabla p = \nabla \cdot \left(\rho \vec{U}\vec{U}\right) - \frac{\partial\left(\rho \vec{U}\right)}{\partial t} - \nabla \cdot \left(\rho \vec{U}\vec{U}\right) = -\frac{\partial\left(\rho \vec{U}\right)}{\partial t}. \tag{C.6}$$

Inserting Eq. (C.6) into the surface integrals of Eqs. (C.3) and (C.4), and inserting them into (C.2) we obtain for the final weak formulation with the moment method for the Lighthill's equation

$$\begin{aligned} &\int_V w_j \frac{1}{c^2}\frac{\partial^2 p_\phi}{\partial t^2}\,\mathrm{d}V + \int_V \nabla\left(w_j\right)\cdot \nabla p_\phi\,\mathrm{d}V \\ &= -\int_V \nabla w_j \cdot \nabla \cdot \overline{\overline{T}}_L\,\mathrm{d}V - \oint_S w_j \vec{e}_n \cdot \frac{\partial\left(\rho \vec{U}\right)}{\partial t}\mathrm{d}S,\ j = 1\ldots N. \end{aligned} \tag{C.7}$$

All assumptions made in arriving to the equation above are also included in the derivation of the basic equation of Lighthill's analogy [1].

Appendix D: Adjoint Lighthill's equation in frequency domain

From Eq. (B.2) the Lighthill's equation can be written in frequency domain as

$$\nabla^2 p + k^2 p = -\nabla\nabla : \overline{\overline{T}}_L , \tag{D.1}$$

where $k = \omega/c$. Now it can be seen that the terms in the general differential equation (A.1) in the Lighthill's analogy are

$$\begin{aligned} f &= p \\ L &= \nabla^2 + k^2 \\ g &= -\nabla\nabla : \overline{\overline{T}}_L . \end{aligned} \tag{D.2}$$

From the second Green's identity (E.4) we obtain ($u = h$)

$$\int_V h\nabla^2 p \,\mathrm{d}V - \oint_S h\vec{e}_n \cdot \nabla p \,\mathrm{d}S = \int_V p\nabla^2 h \,\mathrm{d}V - \oint_S p\vec{e}_n \cdot \nabla h \,\mathrm{d}S . \tag{D.3}$$

Substituting the Laplace operator above by operator L we obtain further

$$\begin{aligned} &\int_V h\left(\nabla^2 p + k^2 p\right)\mathrm{d}V - \oint_S h\vec{e}_n \cdot \nabla p \,\mathrm{d}S \\ &= \int_V p\left(\nabla^2 h + k^2 h\right)\mathrm{d}V - \oint_S p\vec{e}_n \cdot \nabla h \,\mathrm{d}S + \\ &\quad + \int_V \left(hk^2 p - pk^2 h\right)\mathrm{d}V \\ &= \int_V p\left(\nabla^2 h + k^2 h\right)\mathrm{d}V - \oint_S p\vec{e}_n \cdot \nabla h \,\mathrm{d}S . \end{aligned} \tag{D.4}$$

If the boundary condition is presented by the normal component of the boundary velocity v, one obtains from Eq. [1, (B.1)] in frequency domain

$$-\vec{e}_n \cdot \nabla p = \mathrm{j}\omega\rho v \text{ at boundary } S. \tag{D.5}$$

Now the terms in the general boundary condition are

$$\begin{aligned} B &= -\vec{e}_n \cdot \nabla \\ s &= j\omega\rho v . \end{aligned} \tag{D.6}$$

Comparing Eq. (A.6) with definitions (D.2) and (D.6), and Eq. (D.4), one can notice that in this case operator $B = 1$ and the problem is self-adjoint

$$L^a = L \quad B^a = B \quad C^a = C = 1 . \tag{D.7}$$

Appendix E: Green's identities in integral forms

Green's first identity

Consider two scalar functions *u* and *v*. Let *V* be a volume, *S* its boundary and $\vec{e}_n$ a unit normal vector at the boundary pointing outwards the surface, see Figure E1. By utilizing partial integration and the Gauss' theorem one can readily write

$$\begin{aligned}\int_V u\nabla^2 v\,\mathrm{d}V &= \int_V \nabla\cdot(u\nabla v)\mathrm{d}V - \int_V \nabla u\cdot\nabla v\,\mathrm{d}V \\ &= \oint_S u\vec{e}_n\cdot\nabla v\,\mathrm{d}S - \int_V \nabla u\cdot\nabla v\,\mathrm{d}V\,.\end{aligned} \tag{E.1}$$

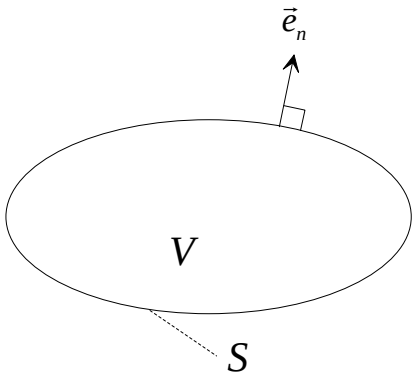

Figure E1. Volume *V*, its boundary *S* and unit normal vector at boundary.

Similarly if the scalar *v* is replaced by a dyadic $\overline{\overline{V}}$

$$\begin{aligned}\int_V u\nabla:\overline{\overline{V}}\,\mathrm{d}V &= \int_V u\nabla\cdot\nabla\cdot\overline{\overline{V}}\,\mathrm{d}V = \int_V \nabla\cdot\left(u\nabla\cdot\overline{\overline{V}}\right)\mathrm{d}V - \int_V \nabla u\cdot\nabla\cdot\overline{\overline{V}}\,\mathrm{d}V \\ &= \oint_S u\vec{e}_n\cdot\nabla\cdot\overline{\overline{V}}\,\mathrm{d}S - \int_V \nabla u\cdot\nabla\cdot\overline{\overline{V}}\,\mathrm{d}V\,.\end{aligned} \tag{E.2}$$

Green's second identity

When *u* and *v* are interchanged in Eq. (E.1) we obtain

$$\int_V v\nabla^2 u\,\mathrm{d}V = \oint_S v\vec{e}_n\cdot\nabla u\,\mathrm{d}S - \int_V \nabla v\cdot\nabla u\,\mathrm{d}V\,. \tag{E.3}$$

Whe Eqs. (E.1) and (E.3) are combined, we obtain the Green's second identity

$$\int_V u\nabla^2 v\,\mathrm{d}V - \int_V v\nabla^2 u\,\mathrm{d}V = \oint_S u\vec{e}_n\cdot\nabla v\,\mathrm{d}S - \oint_S v\vec{e}_n\cdot\nabla u\,\mathrm{d}S \tag{E.4}$$

Appendix F: Möhring's analogy

Möhring's analogy is an enthalpy-based analogy where the stagnation enthalpy B is used as the basic field quantity. It is here derived mathematically in detail to clarify what must be assumed and at what stage, to obtain the required equation, to allow its applicability to be extended when necessary.

To derive the equation for the analogy, we can first manipulate the total time derivative of the stagnation enthalpy according to Eq. [1, (A.8)]

$$\frac{\mathrm{d}B}{\mathrm{d}t} = \frac{1}{\rho}\frac{\mathrm{d}P}{\mathrm{d}t} + T\frac{\mathrm{d}S}{\mathrm{d}t} + \vec{U}\cdot\frac{\mathrm{d}\vec{U}}{\mathrm{d}t}, \tag{F.1}$$

where P is the pressure, ρ is the density, T is the temperature, S is the entropy, $\vec{U}$ is the particle velocity and t is the time variable.

The first term in the right hand side of Eq. (F.1) can be presented by the help of Eqs. [1, (2)] and [1, (B.1)] as

$$\frac{1}{\rho}\frac{\mathrm{d}P}{\mathrm{d}t} = \frac{1}{\rho}\left(\frac{\partial P}{\partial t} + \vec{U}\cdot\nabla P\right) = \frac{1}{\rho}\frac{\partial P}{\partial t} - \vec{U}\cdot\frac{\mathrm{d}\vec{U}}{\mathrm{d}t} + \frac{1}{\rho}\vec{U}\cdot\left(\nabla\cdot\overline{\overline{\sigma}}_{\mu} + \vec{F} - \nabla\cdot\overline{\overline{T}}\right), \tag{F.2}$$

where $\vec{U}$ is the particle velocity, $\overline{\overline{\sigma}}_{\mu}$ is the viscous part of the stress dyadic, $\vec{F}$ is the strength of the force source distribution (dipole distribution + gravitation), and $\overline{\overline{T}}$ is the strength of the momentum source distribution (quadrupole distribution), see [1].

The second term in the right hand side of Eq. (F.1) can be presented by the help of the entropy version of the energy equation [1, (D.1)] as

$$T\frac{\mathrm{d}S}{\mathrm{d}t} = \frac{1}{\rho}\left(\overline{\overline{\sigma}}_{\mu} : \overline{\overline{E}} + \nabla\cdot\left(K\nabla T\right) + \frac{\mathrm{d}\varepsilon}{\mathrm{d}t}\right), \tag{F.3}$$

where S is the entropy, $\overline{\overline{E}}$ is the rate-of-strain dyadic, K is the thermal conductivity of the fluid and ε is the energy per unit volume delivered by the heat source distribution, see [1].

The first term in the parenthesis of the right hand side of Eq. (F.3) can be further presented by the help of Eqs. [1, (B.3)] and [1, (R.16)] as

$$\overline{\overline{\sigma}}_{\mu} : \overline{\overline{E}} = \overline{\overline{\sigma}}_{\mu} : \tfrac{1}{2}\left[\nabla\vec{U} + \left(\nabla\vec{U}\right)_{\mathrm{T}}\right] = \overline{\overline{\sigma}}_{\mu} : \nabla\vec{U} = \nabla\cdot\left(\overline{\overline{\sigma}}_{\mu}\cdot\vec{U}\right) - \vec{U}\cdot\left(\nabla\cdot\overline{\overline{\sigma}}_{\mu}\right), \tag{F.4}$$

where also the symmetry of the dyadic $\overline{\overline{\sigma}}_{\mu}$ has been utilized, in which case

$$\overline{\overline{\sigma}}_{\mu} : \nabla\vec{U} = \left(\overline{\overline{\sigma}}_{\mu}\right)_{\mathrm{T}} : \left(\nabla\vec{U}\right)_{\mathrm{T}} = \overline{\overline{\sigma}}_{\mu} : \left(\nabla\vec{U}\right)_{\mathrm{T}}, \tag{F.5}$$

where subscript T outside the brackets (·) means that the dyadic inside the brackets is transposed.

Inserting Eq. (F.4) into Eq. (F.3) and then inserting Eqs. (F.3) and (F.2) into Eq. (F.1) multiplied by ρ one obtains

$$\begin{aligned}\rho\frac{\mathrm{d}B}{\mathrm{d}t} &= \frac{\partial P}{\partial t} - \rho\vec{U}\cdot\frac{\mathrm{d}\vec{U}}{\mathrm{d}t} + \vec{U}\cdot\left(\nabla\cdot\overline{\overline{\sigma}}_{\mu} + \vec{F} - \nabla\cdot\overline{\overline{T}}\right) + \\ &+ \nabla\cdot\left(\overline{\overline{\sigma}}_{\mu}\cdot\vec{U}\right) - \vec{U}\cdot\left(\nabla\cdot\overline{\overline{\sigma}}_{\mu}\right) + \nabla\cdot\left(K\nabla T\right) + \frac{\mathrm{d}\varepsilon}{\mathrm{d}t} + \rho\vec{U}\cdot\frac{\mathrm{d}\vec{U}}{\mathrm{d}t} \\ &= \frac{\partial P}{\partial t} + f_{ds},\end{aligned} \tag{F.6}$$

where

$$\begin{aligned} f_{ds} &= f_d + f_s \\ f_d &= \nabla\cdot\left(\vec{U}\cdot\overline{\overline{\sigma}}_{\mu} + K\nabla T\right) \\ f_s &= \left[\vec{U}\cdot\left(\vec{F} - \nabla\cdot\overline{\overline{T}}\right) + \frac{\mathrm{d}\varepsilon}{\mathrm{d}t}\right]. \end{aligned} \tag{F.7}$$

The general state equation [1, (C.1)] with [1, (C.2)] when applied to ρ(*P*,*S*) can be written as

$$\mathrm{d}\rho = \left(\frac{\partial\rho}{\partial P}\right)_S \mathrm{d}P + \left(\frac{\partial\rho}{\partial S}\right)_P \mathrm{d}S = \frac{1}{c^2}\mathrm{d}P + \left(\frac{\partial\rho}{\partial S}\right)_P \mathrm{d}S, \tag{F.8}$$

where also the definition of the local speed of sound *c* in constant entropy [1, (A.4)] has been used. The subscript *S* or *P* outside the brackets (·) means that respectively the entropy or the pressure is held constant during the operation inside the brackets.

Now the continuity equation [1, (A.1)]

$$\frac{\partial\rho}{\partial t} + \nabla\cdot\left(\rho\vec{U}\right) = \rho q, \tag{F.9}$$

where *q* is the strength of the mass source distribution (monopole distribution, volume velocity distribution), can be written as

$$\frac{1}{c^2}\frac{\partial P}{\partial t} + \left(\frac{\partial\rho}{\partial S}\right)_P \frac{\partial S}{\partial t} + \nabla\cdot\left(\rho\vec{U}\right) = \rho q. \tag{F.10}$$

Taking term $\partial P/\partial t$ from Eq. (F.6) as

$$\frac{\partial P}{\partial t} = \rho \frac{\mathrm{d}\, B}{\mathrm{d}\, t} - f_{ds} \tag{F.11}$$

and inserting it to Eq. (F.10) one obtains

$$\frac{\rho}{c^2}\frac{\mathrm{d}\, B}{\mathrm{d}\, t} + \nabla \cdot \left(\rho \vec{U}\right) = -\left(\frac{\partial \rho}{\partial S}\right)_P \frac{\partial S}{\partial t} + \frac{1}{c^2} f_{ds} + \rho q\,. \tag{F.12}$$

The enthalpy version of the Navier-Stokes equation [1, (B.13)] with [1, (B.12)]

$$\frac{\partial \vec{U}}{\partial t} = -\nabla B - \vec{\omega} \times \vec{U} + T\nabla S + \frac{1}{\rho}\left(\nabla \cdot \overline{\overline{\sigma}}_\mu + \vec{F} - \nabla \cdot \overline{\overline{T}}\right), \tag{F.13}$$

where $\vec{\omega}$ is the vorticity distribution

$$\vec{\omega} = \nabla \times \vec{U}\,. \tag{F.14}$$

Multiplying the Navier-Stokes equation (F.13) with density we obtain utilizing Eqs. (F.8) and (F.11)

$$\begin{aligned}\frac{\partial\left(\rho \vec{U}\right)}{\partial t} &= \vec{U}\frac{\partial \rho}{\partial t} - \rho\nabla B - \rho\vec{\omega}\times\vec{U} + \rho T\nabla S + \nabla \cdot \overline{\overline{\sigma}}_\mu + \vec{F} - \nabla \cdot \overline{\overline{T}} \\ &= \frac{\rho \vec{U}}{c^2}\frac{\mathrm{d}\, B}{\mathrm{d}\, t} - \frac{\vec{U}}{c^2} f_{ds} + \vec{U}\left(\frac{\partial \rho}{\partial S}\right)_P \frac{\partial S}{\partial t} \\ &\quad - \rho\nabla B - \rho\vec{\omega}\times\vec{U} + \rho T\nabla S + \nabla \cdot \overline{\overline{\sigma}}_\mu + \vec{F} - \nabla \cdot \overline{\overline{T}}\,.\end{aligned} \tag{F.15}$$

Taking the time derivative of Eq. (F.12) and the divergence of Eq. (F.15) we obtain

$$\begin{aligned}&\frac{\partial}{\partial t}\left(\frac{\rho}{c^2}\frac{\mathrm{d}\, B}{\mathrm{d}\, t}\right) + \nabla \cdot \left(\frac{\rho \vec{U}}{c^2}\frac{\mathrm{d}\, B}{\mathrm{d}\, t} - \rho\nabla B\right) \\ &= \nabla \cdot \left(\rho\vec{\omega}\times\vec{U}\right) - \nabla \cdot \left(\rho T\nabla S\right) - \frac{\partial}{\partial t}\left[\left(\frac{\partial \rho}{\partial S}\right)_P \frac{\partial S}{\partial t}\right] - \nabla \cdot \left[\vec{U}\left(\frac{\partial \rho}{\partial S}\right)_P \frac{\partial S}{\partial t}\right] + \\ &\quad + \frac{\partial}{\partial t}\frac{f_{ds}}{c^2} + \nabla \cdot \left(\frac{\vec{U}}{c^2} f_{ds}\right) - \nabla\nabla : \overline{\overline{\sigma}}_\mu + \\ &\quad + \frac{\partial}{\partial t}(\rho q) - \nabla \cdot \vec{F} + \nabla\nabla : \overline{\overline{T}}\,.\end{aligned} \tag{F.16}$$

In the case of no mass, heat, force or momentum source distributions this leads to

$$\begin{aligned}&\frac{\partial}{\partial t}\left(\frac{\rho}{c^2}\frac{\mathrm{d}B}{\mathrm{d}t}\right)+\nabla\cdot\left(\frac{\rho\vec{U}}{c^2}\frac{\mathrm{d}B}{\mathrm{d}t}-\rho\nabla B\right)\\ =\nabla\cdot\left(\rho\vec{\omega}\times\vec{U}\right)&-\nabla\cdot\left(\rho T\nabla S\right)-\frac{\partial}{\partial t}\left[\left(\frac{\partial\rho}{\partial S}\right)_P\frac{\partial S}{\partial t}\right]-\nabla\cdot\left[\vec{U}\left(\frac{\partial\rho}{\partial S}\right)_P\frac{\partial S}{\partial t}\right]+\\ &+\frac{\partial}{\partial t}\frac{f_d}{c^2}+\nabla\cdot\left(\frac{\vec{U}}{c^2}f_d\right)-\nabla\nabla:\overline{\overline{\sigma}}_\mu .\end{aligned}\qquad\text{(F.17)}$$

If further there are no viscous or thermal losses, we arrive to the equation of Möhring's analogy

$$\begin{aligned}&\frac{\partial}{\partial t}\left(\frac{\rho}{c^2}\frac{\mathrm{d}B}{\mathrm{d}t}\right)+\nabla\cdot\left(\frac{\rho\vec{U}}{c^2}\frac{\mathrm{d}B}{\mathrm{d}t}-\rho\nabla B\right)\\ =\nabla\cdot\left(\rho\vec{\omega}\times\vec{U}\right)&-\nabla\cdot\left(\rho T\nabla S\right)-\frac{\partial}{\partial t}\left[\left(\frac{\partial\rho}{\partial S}\right)_P\frac{\partial S}{\partial t}\right]-\nabla\cdot\left[\vec{U}\left(\frac{\partial\rho}{\partial S}\right)_P\frac{\partial S}{\partial t}\right].\end{aligned}\qquad\text{(F.18)}$$